# Onset of Pulsing in Two-Phase Cocurrent Downflow through a Packed Bed

In cocurrent downflow of a gas and a liquid through a packed column, a transition from trickling flow to pulsing flow is observed as one increases the flow rates. A simple macroscopic model for the two-phase flow is analyzed to examine whether this regime transition should be viewed as the loss of stability of a steady state or the loss of existence of any solution for the steady-state equations of motion. The former appears to be a more reasonable interpretation and an explicit algebraic criterion for the onset of pulsing is presented.

**K. Grosser and R. G. Carbonell**
Department of Chemical Engineering
North Carolina State University
Raleigh, NC 27695

**S. Sundaresan**
Department of Chemical Engineering
Princeton University
Princeton, NJ 08544

## Introduction

Trickle bed reactors, in which a gas and a liquid flow concurrently downwards through a packed column, are being used extensively in the chemical and petroleum industries for such reactions as hydrodesulfurization, hydrocracking, oxidation and hydrogenation (Satterfield, 1975; Herskowitz and Smith, 1983). Several different hydrodynamic regimes are possible for nonfoaming flow in trickle beds (Charpentier, 1976; Midoux et al., 1976), the two most commonly encountered being trickle flow which is obtained at low liquid and gas flowrates, and pulsing flow at high gas and liquid flowrates. The trickle flow is characterized by the existence of rivulets of liquid flowing over the packing, while in pulsing flow alternate bands of liquid-rich and gas-rich regions traverse the bed. Although most laboratory and pilot scale trickle beds operate in the trickle flow regime, commercial petroleum processing operations such as hydrodesulfurization and hydrotreating often reach the pulsing flow regime (Charpentier and Favier, 1975; Charpentier et al., 1971). The recent development of more active catalysts is pushing commercial operations towards and into the pulsing flow regime (Blok and Drinkenburg, 1982a; Lerou et al., 1980).

The knowledge of the flow regime that will be encountered at a given set of flow conditions is very important for the design of a trickle bed reactor. Variables such as the liquid holdup, pressure drop *and mass transfer* coefficients change significantly, depending on the regime in which a reactor is operated (Charpentier and Favier, 1975; Gianetto et al., 1973, 1978; Kobayashi et al., 1979; Specchia et al., 1974). The overall bed pressure drop, in particular, can increase by up to a factor of two upon transition from trickling to pulsing (Schmidt and Clements, 1977).

The early approaches to correlate the conditions at which this regime transition occurs relied heavily on empirical flow regime maps (Beimesch and Kessler, 1971; Charpentier et al., 1971; Charpentier and Favier, 1975; Chou et al., 1977; Fukushima and Kusaka, 1977; Gianetto et al., 1973, 1978; Larkins et al., 1961; Sato et al., 1973; Satterfield, 1975; Specchia et al., 1974, 1977; Talmor, 1977; Tosun, 1984; Turpin and Huntington, 1967; Weekman and Myers, 1964). There is as of yet no real consensus on the underlying mechanisms which dominate the transition from trickling to pulsing flow.

Many parameters should be considered in a physical model of the transition mechanism. These include the mass flow rates of the liquid and gas phases, the viscosities and densities of the liquid and the gas, the interfacial tension, the size, porosity and wettability of the packing particles, and the column width and height. A number of studies (Chou et al., 1977; Kobayashi et al., 1979; Morsi et al., 1978, 1980, 1984; Sicardi et al., 1979; Sicardi and Hofmann, 1980) have pointed out the importance of the effects of the physical properties of the fluids on the transition from the trickling flow to the pulsing flow regime. Sicardi and Hofmann (1980) noted the possible effects of the particle size and shape, surface roughness, gas-liquid interfacial tension and the ratio of the particle-to-reactor diameter. Chou et al. (1977) indicated that an increased particle wettability caused transition to occur at higher flow rates. These investigators also demonstrated significant effects of the packing porosity and the interfacial tension on the transition from trickling to pulsing flow. Of these parameters, the interfacial tension, the liquid viscosity, the densities of the gas and the liquid, and the packing porosity have been incorporated into flow maps empirically (Baker, 1954; Gianetto et al., 1973; Satterfield, 1975). But, as pointed out by Chou et al. (1977) these flow map parameters have no theoretical basis as they were proposed originally for two-phase flow maps in horizontal pipes by Baker (1954).

Correspondence concerning this paper should be addressed to S. Sundaresan.

Several explanations for the inception of pulsing have been hypothesized. Blok et al. (1983) have proposed on the basis of their experimental observations that when the liquid-phase Froude number exceeds a certain threshold value, a transition from trickling to pulsing flow results. A fundamental explanation of why this should be the case remains to emerge. Further, this model does not consider the effect of interfacial tension on the trickling-to-pulsing transition.

Sicardi et al. (1979) and Sicardi and Hofmann (1980) proposed that the transition from trickling to pulsing be physically interpreted as being due to the formation of waves with large amplitudes which occlude the packing channel and suggested a semiempirical correlation for this transition. Ng (1986) has presented a more detailed analysis of this "occlusion" concept. He has also compared the results of this microscopic theory with some experimental flow map data, and demonstrated qualitative agreement. These studies, which attempt to explain the trickling-to-pulsing transition on the basis of a microscopic view of the gas-liquid flow in the channels, do not address the issue as to why these microscopic occlusions of the various flow channels should synchronize to yield the macroscopically nonuniform behavior of pulsing.

In contrast to the above microscopic approach, we shall adopt a macroscopic view of the two-phase flow in the packed column. Two possible physical interpretations of the trickling-to-pulsing transition will be examined.

If the feed gas and feed liquid are distributed uniformly at the top of a uniformly packed column and if we treat both the phases as incompressible, then a uniform state where the liquid holdup and the pressure gradient are essentially spatially uniform will be obtained in the trickling regime. We shall investigate the stability of this uniform state and derive a condition for the onset of instability.

Strictly speaking, the state obtained in the trickling regime is not spatially uniform. As the gas travels down the column, its volumetric flow rate increases steadily, and this will give rise to a gradual (although very small) decrease in the liquid holdup. It will be shown later that this gradual variation in the liquid holdup sets up a competition between the inertial and capillary forces and that it would not be possible to obtain steady-state solutions for the two-phase flow model equations under certain conditions. The loss of existence of a solution for the steady-state equations for the cocurrent downflow in a packed column may imply the onset of a time-dependent solution, i.e., the trickling-to-pulsing transition. A significant feature of this model for the onset of pulsing is that it can bring out the effect of column length on the conditions at which pulsing will first appear.

As will be shown later, the loss of stability of a steady state (first scenerio above) occurs at lower gas and liquid flow rates than the loss of existence of a steady state (second scenerio above). In this section, we shall also compare the predictions of these models with the experimental data on trickling-to-pulsing transition and the microscopic model of Ng (1986).

## Stability of Cocurrent Flow of Two Incompressible Fluids

### *Macroscopic model for the two-phase flow*

Consider a column which is packed uniformly with a void fraction $\epsilon$. We shall focus our attention on a column of large cross sectional area so that we need not be concerned with the wall effects. As mentioned earlier, we shall assume here that the gas phase is incompressible. Let $G$ and $L$ denote the mass fluxes of the gas and liquid through the column (in kg/m$^2$ · s), respectively. It can be easily shown that the macroscopic (volume-averaged) continuity and momentum balance equations are:

$$\epsilon_\ell + \epsilon_g = \epsilon \tag{1}$$

$$\frac{\partial \epsilon_i}{\partial t} + \nabla \cdot (\epsilon_i u_i) = 0, \quad i = \ell, g \tag{2}$$

$$\rho_i \epsilon_i \left\{ \frac{\partial u_i}{\partial t} + u_i \cdot \nabla u_i \right\} = -\epsilon_i \nabla p_i + \epsilon_i \rho_i g + \underline{F}_i + \nabla \cdot [\epsilon_i \underline{\underline{\tau}}_i + \epsilon_i \underline{\underline{R}}_i], \quad i = \ell, g. \tag{3}$$

Here $\epsilon_i$, $i = \ell, g$ denote the fraction of the bed volume occupied by the liquid and gas, respectively; $\underline{u}_i$, $i = \ell, g$ are the interstitial velocities of these two phases; $\rho_i$, $i = \ell, g$ are the mass densities of the two phases, and $p_i$, $i = \ell, g$ are the pressures in the two phases. $\underline{F}_i$, $i = \ell, g$ denote the total drag force per unit bed volume experienced by the liquid and gas, respectively, and $g$ is the acceleration due to gravity. $\underline{\underline{\tau}}_i$ and $\underline{\underline{R}}_i$ denote the volume-averaged viscous stress tensor and the pseudoturbulence stress tensor of phase $i$, respectively. The pseudoturbulence tensor (which is analogous to the Reynolds stress tensor in turbulence) arises because the local velocities of the phases are in general different from the volume-averaged velocities. Through a scaling analysis it is easy to argue that the viscous and pesudoturbulence terms on the righthand side of Eq. 3 are small compared to the drag force term. Hence we shall neglect these two terms in the analyses presented in this paper.

In addition to Eqs. 1 to 3, one can set up a further relationship between $p_g$ and $p_\ell$ by volume-averaging the stress balance at the gas-liquid interface. We propose that the capillary pressure, $p_c$ ($= p_g - p_\ell$), be assumed to be adequately represented by the well-known Leverett's $J$ function (1941)

$$p_c = \left(\frac{\epsilon}{k}\right)^{1/2} \sigma J(\epsilon_\ell) \tag{4}$$

where $k$ is the permeability of the packed column and $\sigma$ is the gas-liquid interfacial tension.

The above representation for the capillary pressure has found extensive use in the analysis of multiphase flow through porous media (Dullien, 1979; Scheidegger, 1974). However, the validity of such a representation for trickle beds has not been established so far. Yet, one may argue that the $J$-function approach to describing the variations in the capillary pressure is not unrealistic for the present problem.

In porous media applications (for which Eq. 4 was originally developed) it is well known that the capillary pressure exhibits pronounced hysteresis behavior. This hysteresis is usually attributed to a hysteresis in the contact angle. An immediate consequence of this capillary pressure hysteresis is the hysteresis behavior in the relative permeabilities of the flowing fluids (Dullien, 1979; Scheidegger, 1974). This hysteresis in the relative permeabilities is manifested by a history dependence of the pressure gradient required to maintain specified throughputs for the two fluids.

One can therefore make the following requirement. If the $J$-

function approach to describe the capillary pressure is to be a tolerable first approximation in the context of trickle beds, then the pressure gradient required to maintain specified throughputs of the gas and the liquid in the trickle bed must exhibit a history dependence. Such indeed happens to be the case. The history dependence of the pressure gradient in the trickling region is now well documented (Kan and Greenfield, 1978, 1979; Levec et al., 1984, 1986, 1988; Christensen et al., 1986) and, in fact, this history dependence is strikingly similar to that observed in porous media applications. It is this similarity which leads us to hope that the dependence of the capillary pressure on the operating conditions is captured in an adequate fashion for the most part by the $J$ function.

It has been shown by Saez and Carbonell (1985) that constitutive models for $\underline{F}_i$, $i = \ell, g$, based on the relative permeability concept correlate a wide range of pressure gradient and liquid holdup data in the trickling regime reasonably satisfactorily. We shall employ these constitutive models in our analysis, while noting that the analysis described below can be easily adapted for any other set of constitutive models.

$$\underline{F}_g = -\left\{\frac{A\mu_g(1-\epsilon)^2\epsilon^{1.8}}{d_e^2\epsilon_g^{2.8}} + \frac{B\rho_g(1-\epsilon)\epsilon^{1.8}|u_g|}{\epsilon_g^{1.8}d_e}\right\}u_g \tag{5}$$

$$\underline{F}_\ell = -\left\{\frac{\epsilon-\epsilon_\ell'}{\epsilon_\ell-\epsilon_\ell'}\right\}^{2.9} \cdot \left\{\frac{A\mu_\ell(1-\epsilon)^2\epsilon_\ell^2}{d_e^2\epsilon^3} + \frac{B\rho_\ell(1-\epsilon)\epsilon_\ell^3|u_\ell|}{\epsilon^3 d_e}\right\}u_\ell \tag{6}$$

Here $d_e$ is the equivalent particle diameter; $\mu_i$, $i = \ell, g$ are the viscosities; $A$ and $B$ are the Ergun constants (equal to 180 and 1.8, respectively). The static (residual) liquid holdup, $\epsilon_\ell'$, is estimated from (Saez and Carbonell, 1985)

$$\epsilon_\ell' = (20 + 0.9E\ddot{o}^*)^{-1}$$

where

$$E\ddot{o}^* = \frac{\rho_\ell g d_e^2\epsilon^2}{\sigma(1-\epsilon)^2}. \tag{7}$$

Strictly speaking, as the pressure gradient required to maintain specified gas and liquid throughputs in the trickling regime of flow is history-dependent, any general constitutive models for the drag terms $\underline{F}_\ell$ and $\underline{F}_g$ in Eq. 3 should also reflect this history dependence. At the present time, no such constitutive models are available. In fact, most of the data on pressure drop and liquid holdup available in the literature appear to have been gathered with no special attention to the manner in which the flows were established. This should not be viewed too critically as the existence of a systematic history dependence has been recognized only in recent years. Thus the constitutive model of Saez and Carbonell (1985) should be viewed as an average of the behavior observed in the trickling regime.

As the $J(\epsilon_\ell)$ function is multivalued, we must also decide which of these multiple values one should use in the mathematical analysis. In gas-liquid systems the experimentally obtained $J$ values typically lie between two limiting curves, known as the "drainage" and "imbibition" curves. The drainage curve is obtained when the liquid saturation, $s_\ell$ $(=\epsilon_\ell/\epsilon)$ is decreased steadily from its maximum value (which is typically equal to unity in the case of gas-liquid systems). In the context of trickle beds, this may be compared with an experimental sequence in which, starting from zero gas flow rate, one steadily increases the gas flowrate while holding the liquid flowrate constant.

The imbibition curve corresponds to the measurements obtained when the liquid saturation is steadily increased from its residual value, $s_\ell'$ $(=\epsilon_\ell'/\epsilon)$ to unity.

In our analysis let us first consider the $J$ vs. $\epsilon_\ell$ behavior corresponding to the drainage curve. We shall return to this point later on and argue that this drainage curve is indeed the most relevant one for stability considerations. We also note that to be consistent with the Ergun equation used to describe the interphase drag forces, we calculate the permeability of the packed bed according to the relation

$$\left(\frac{\epsilon}{k}\right)^{1/2} = \frac{(1-\epsilon)}{\epsilon d_e}\sqrt{A} \tag{8}$$

### *Steady state characteristics*

For the purpose of the present study, we shall assume that the gas and the liquid are distributed uniformly at the top of the column, so that lateral variations (at a macroscopic level) in the dependent variables do not exist. (It is needless to emphasize that the lateral maldistribution of liquid is an important consideration in trickle bed operations. But an analysis of the effect of such maldistributions on the performance of trickle beds are beyond the scope of this publication.) Then one can write,

$$\epsilon_\ell(z) + \epsilon_g(z) = \epsilon \tag{9}$$

$$\frac{d}{dz}\{\epsilon_i u_{iz}\} = 0, \quad i = \ell, g \tag{10}$$

$$u_{ix} = u_{iy} = 0, \quad i = \ell, g \tag{11}$$

$$\rho_i\epsilon_i u_z\frac{du_{iz}}{dz} = -\epsilon_i\frac{dp_i}{dz} + F_{iz} + \epsilon_i\rho_i g, \quad i = \ell, g \tag{12}$$

$$p_g(z) - p_\ell(z) = \left(\frac{\epsilon}{k}\right)^{1/2}\sigma J[\epsilon_\ell(z)]. \tag{13}$$

Here $x$ and $y$ denote cartesian coordinate directions in the horizontal plane and the $z$ axis is pointing vertically downward; $u_{ix} \cdot u_{iy}$, and $u_{iz}$, $i = \ell, g$ denote the components of the local mean velocity vectors in the various directions. $F_{iz}$, $i = \ell, g$ denote the drag forces acting in the z direction. It is straightforward to combine Eqs. 9–13 and obtain

$$\left\{\frac{G^2}{\rho_g\epsilon_g^3} + \frac{L^2}{\rho_\ell\epsilon_\ell^3} + \left(\frac{\epsilon}{k}\right)^{1/2}\sigma J'(\epsilon_\ell)\right\}\frac{d\epsilon_\ell}{dz} = \left\{\frac{F_{gz}}{\epsilon_g} - \frac{F_{\ell z}}{\epsilon_\ell} + (\rho_g - \rho_\ell)g\right\} \tag{14}$$

where

$$G = \rho_g\epsilon_g u_{gz}, \quad L = \rho_\ell\epsilon_\ell u_{\ell z} \tag{15}$$

are mass fluxes of the gas and liquid through the column, and

$J'(\epsilon_\ell)$ denotes $dJ/d\epsilon_\ell$. Now, for specified throughput rates $G$ and $L$, one can compute a uniform steady state for which $d\epsilon_\ell/dz = 0$, from

$$G = \rho_g \epsilon_g^0 u_{gz}^0, \quad L = \rho_\ell \epsilon_\ell^0 u_{\ell z}^0 \tag{16}$$

$$\frac{F_{gz}^0}{\epsilon_g^0} - \frac{F_{\ell z}^0}{\epsilon_\ell^0} + (\rho_g - \rho_\ell)g = 0 \tag{17}$$

$$\epsilon_g^0 + \epsilon_\ell^0 = \epsilon \tag{18}$$

where $F_{gz}^0$ and $F_{\ell z}^0$ denote the drag forces evaluated at conditions corresponding to the uniform state (indicated by superscript zero).

Although this uniform state may be attained in the middle of the column, (provided the column is sufficiently long), there will, in general, be boundary layers at one or both ends of the column. The terms on the LHS of Eq. 14 may depart appreciably from zero in these boundary layers, but will be small (when compared to each of the terms on the RHS) outside of these regions. It is generally believed that the boundary layers are very thin, of the order of a few particle diameters. The trickle beds used in the laboratory studies are typically very long, containing several hundred particles. The commercial scale units are even longer.

Now strictly speaking, in order to determine the conditions at which trickling-to-pulsing transition occurs according to the model considered here, one must consider small perturbations around the steady state described by Eqs. 9, 14, and 15 and examine the fate of these perturbations. However, as the uniform state appears to prevail over most of the length of the columns typically used in both pilot and commercial scale operations, it is probably adequate to consider small perturbations around the uniform steady state described by Eqs. 16–18 and an infinitely long column to deduce the conditions at which trickling-to-pulsing transition occurs. This assumption is made in the analysis described below. Such an analysis would completely miss the role of the end effects on the conditions of pulsing inception, should such an effect exist.

### *Linear stability of the uniform steady state*

Consider the cocurrent downflow of a gas and a liquid through an infinitely long packed column, whose mechanics are governed by the one-dimensional equations of motion described by Eqs. 9–13. The uniform state described by Eqs. 16–18 is a solution to these equations of motion, and the corresponding axial pressure gradient is given by

$$\left(\frac{dp_g^0}{dz}\right) = \left(\frac{dp_\ell^0}{dz}\right) = \frac{F_{gz}^0}{\epsilon_g^0} + \rho_g g \tag{19}$$

To examine the linear stability of this uniform state, consider one-dimensional perturbations around this uniform state.

$$\begin{aligned} \epsilon_i(z,t) &= \epsilon_i^0 + \epsilon_{i1}(z,t) \\ u_{iz}(z,t) &= u_{iz}^0 + u_{i1}(z,t) \\ p_i(z,t) &= p_i^0(z) + p_{i1}(z,t), \quad i = \ell, g \end{aligned} \tag{20}$$

Introducing these definitions into Eqs. 9–13 and linearizing, one obtains

$$\frac{\partial \epsilon_{i1}}{\partial t} + \epsilon_i^0 \frac{\partial u_{i1}}{\partial z} + u_{iz}^0 \frac{\partial \epsilon_{i1}}{\partial z} = 0, \quad i = \ell, g \tag{21}$$

$$\epsilon_{\ell 1} + \epsilon_{g1} = 0 \tag{22}$$

$$\rho_i \epsilon_i^0 \left\{ \frac{\partial u_{i1}}{\partial t} + u_{iz}^0 \frac{\partial u_{i1}}{\partial z} \right\} = -\epsilon_i^0 \frac{\partial p_{i1}}{\partial z} - \epsilon_{i1} \frac{\partial p_i^0}{\partial z} + \epsilon_{i1}\rho_i g + \alpha_i u_{i1} + \beta_i \epsilon_{i1}, \quad i = \ell, g \tag{23}$$

$$p_{g1} - p_{\ell 1} = \left(\frac{\epsilon}{k}\right)^{1/2} \sigma J'(\epsilon_\ell^0)\epsilon_{\ell 1} \tag{24}$$

where

$$J'(\epsilon_\ell^0) = \left(\frac{dJ}{d\epsilon_\ell}\right)^0 \tag{25}$$

$$\alpha_i = \left(\frac{\partial F_{iz}}{\partial u_i}\right)^0; \quad \beta_i = \left(\frac{\partial F_{iz}}{\partial \epsilon_i}\right)^0, \quad i = \ell, g \tag{26}$$

and we have neglected the viscous and pseudoturbulence stresses.

Following the usual procedure for linear stability analysis, we assume that

$$\begin{aligned} u_{i1} &= \hat{u}_{i1} \exp\{st + j\omega z\} \\ \epsilon_{i1} &= \hat{\epsilon}_{i1} \exp\{st + j\omega z\} \\ p_{i1} &= \hat{p}_{i1} \exp\{st + j\omega z\} \end{aligned} \tag{27}$$

where $j = \sqrt{-1}$. Introducing Eq. 27 into Eqs. 21–24 and simplifying, we obtain

$$W_1 s^2 + s(W_2 + 2j\omega W_3) - \omega^2 W_4 - j\omega W_5 = 0 \tag{28}$$

where

$$W_1 = \frac{\rho_g}{\epsilon_g^0} + \frac{\rho_\ell}{\epsilon_\ell^0} \tag{29}$$

$$W_2 = -\frac{\alpha_\ell}{(\epsilon_\ell^0)^2} - \frac{\alpha_g}{(\epsilon_g^0)^2} \tag{30}$$

$$W_3 = \frac{\rho_g u_{gz}^0}{\epsilon_g^0} + \frac{\rho_\ell u_{\ell z}^0}{\epsilon_\ell^0} \tag{31}$$

$$W_4 = \frac{\rho_g (u_{gz}^0)^2}{\epsilon_g^0} + \frac{\rho_\ell (u_{\ell z}^0)^2}{\epsilon_\ell^0} + \left(\frac{\epsilon}{k}\right)^{1/2} \sigma J'(\epsilon_\ell^0) \tag{32}$$

$$W_5 = \frac{F_{\ell z}^0}{(\epsilon_\ell^0)^2} + \frac{F_{gz}^0}{(\epsilon_g^0)^2} - \frac{\beta_\ell}{\epsilon_\ell^0} - \frac{\beta_g}{\epsilon_g^0} + \frac{\alpha_\ell u_{\ell z}^0}{(\epsilon_\ell^0)^2} + \frac{\alpha_g u_{gz}^0}{(\epsilon_g^0)^2} \tag{33}$$

It follows from Eq. 28 that

$$s = \frac{(-W_2 \pm Y_1)}{2W_1} + j\frac{(-2\omega W_3 \pm Y_2)}{2W_1} \tag{34}$$

where $Y_1 = Y_1(\omega)$ and $Y_2 = Y_2(\omega)$ are given by

$$Y_1 + jY_2 = \sqrt{W_2^2 + 4\omega^2(W_1W_4 - W_3^2) + 4j\omega(W_2W_3 + W_1W_5)} \quad (35)$$

By requiring the real part of $s$ to be less than or equal to zero for stability, one obtains

$$W_1W_5^2 + 2W_2W_3W_5 + W_2^2W_4 \leq 0. \quad (36)$$

The condition for the trickling-to-pulsing transition then becomes

$$W_1W_5^2 + 2W_2W_3W_5 + W_2^2W_4 = 0. \quad (37)$$

In order to determine the liquid flowrate corresponding to the trickling-to-pulsing transition for a specified gas flow rate (or vice versa) one must solve Eqs. 16–18 and 37.

Now, in order to use the stability criterion (Eq. 37) for locating the trickling-to-pulsing transition curve, one must know the values of $J'(\epsilon_\ell)$, $\epsilon_\ell' < \epsilon_\ell < \epsilon$. As mentioned earlier, the $J$ function is multivalued. Even when we restrict our attention to the so-called drainage curve, the $J$ function is not known quantitatively, especially for beds of large particles (such as those used in trickle bed operations). From experimental results carried out in porous media (Leverett, 1941), we may speculate the qualitative form of this $J$ function. In general, $J$ is large for small values of $\epsilon_\ell$. As $\epsilon_\ell$ is increased, $J$ decreases rapidly at first and then at a much slower rate for intermediate values of $\epsilon_\ell$. Finally as $\epsilon_\ell \to \epsilon$, it decreases rapidly again towards zero. The expression

$$J(s_\ell) = 0.48 + 0.036 \ln\left(\frac{1 - s_\ell}{s_\ell}\right) \quad (38)$$

describes the $J$-function data of Leverett (1941) reasonably well, Figure 1. The agreement between the data and Eq. 38 is not very good at very low and very high values of liquid saturation. This is not of great concern as the liquid holdup values typically encountered in trickle beds (especially at conditions near trickling-to-pulsing transition observed experimentally) correspond to the intermediate plateau region of the $J$ function.

Let us first consider whether the capillary pressure does indeed play any significant role in the stability of the uniform state in the trickle beds. To see this, let us suppose that $\sigma = 0$ so that the capillary pressure term vanishes. Then, one can readily show that the uniform state is always unstable, i.e., the inequality (Eq. 36) is always satisfied for every $G > 0$ and $L > 0$. This is of course not borne out by experiments. When $\sigma > 0$, one can readily show from the inequality (Eq. 36) that a necessary (but not sufficient) condition for this inequality to be feasible is that $J'(\epsilon_\ell^0) < 0$. Experimental measurements of the capillary pressure (Leverett, 1941) and Eq. 38 do indeed show that $J'(\epsilon_\ell) < 0$.

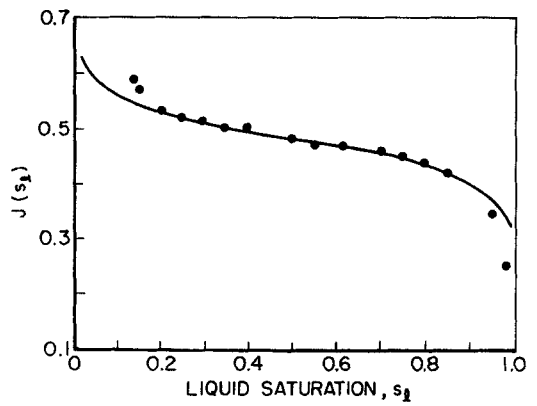


**Figure 1. Variation of $J$ as a function of $s_\ell$.**
●, Data of Leverett (1941); —, Eq. 38.

**Table 1. Parameter Values Used in the Simulations**

| | |
|---|---|
| $A = 180$ | $\sigma = 7.15 \times 10^{-2}$ kg/s$^2$ |
| $B = 1.8$ | $\rho_g = 1.17$ kg/m$^3$ |
| $d_e = 0.003$ m | $\rho_\ell = 10^3$ kg/m$^3$ |
| $g = 9.8$ m/s$^2$ | $\mu_g = 1.84 \times 10^{-5}$ kg/m · s |
| $\epsilon = 0.37$ | $\mu_\ell = 10^{-3}$ kg/m · s |

Physically (according to the model) the inertial terms are inherently destabilizing the uniform steady state and it is the capillary pressure term which is opposing this destabilizing effect and is rendering stability to the uniform state for some two-phase flow conditions. As $G$ and/or $L$ is increased, the destabilizing effect of the inertial terms becomes more pronounced and at sufficiently large flowrates the capillary pressure term can no longer compensate the destabilizing inertial forces. It is therefore clear that the capillary pressure term must be accounted for in the model in order to predict the trickling-to-pulsing transition satisfactorily.

In the analysis described in this paper we have used Eq. 38 as a constitutive model for the $J$ function. Using this functional dependence for $J$ and the parameter values presented in Table 1, the trickling-to-pulsing transition curve (as predicted by Eq. 37) for the air-water system in a bed packed with 3 mm beads is presented in Figure 2. Also shown for comparison are the experimental results of Christensen et al. (1986) and the predictions of the correlation by Charpentier and Favier (1975). The agreement between the experimental results and the prediction of the stability criterion is very encouraging when we consider the fact

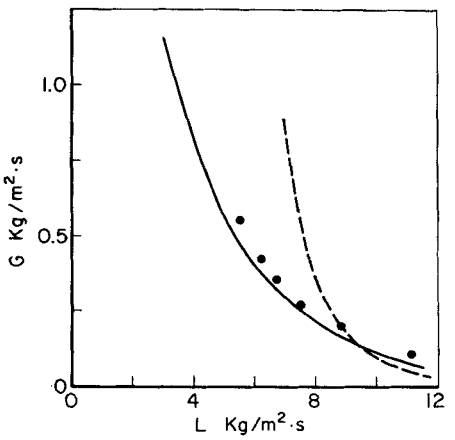


**Figure 2. Trickling-to-pulsing transition curve for the air-water system.**
—, obtained by solving Eqs. 16–18 and 37; – – –, prediction of the correlation due to Charpentier and Favier (1975); ●, experimental data of Christensen et al. (1986). The parameter values are given in Table 1.

that the model has no adjustable parameters. A more detailed comparison of the predictions of this model with the literature data on trickling-to-pulsing transition and the predictions of the microscopic model of Ng (1986) will be described later in Section 4.

### *Capillary pressure function*

It was discussed earlier that the capillary pressure function is multivalued. In the results presented above we have used the $J$-function relationship corresponding to the so-called drainage curve. One can easily repeat the analysis using the $J$-function relationship corresponding to the imbibition curve or any curve bounded by the drainage and imbibition curves. By doing this one would generate a number of curves in the $G$ vs. $L$ plane representing the trickling-to-pulsing transition, each curve corresponding to a different $J$-function relationship. This raises the issue of selecting the right curve for comparing with experimental results. We believe that the trickling-to-pulsing transition predicted by using the $J$-function relationship corresponding to the drainage curve is the correct choice for reasons given below.

Considering that the transition from the trickling regime to the pulsing regime is one in which a steady hydrodynamic solution loses its stability and becomes unstable, it is quite reasonable to argue that the correct trickling-to-pulsing transition curve which one must use in comparisons with experiments is the one which predicts the loss of stability for the lowest throughputs (i.e., lowest $G$ for a specified $L$ and vice versa). Without delving into the details, we simply state that the $J$-function relationship corresponding to the drainage curve then emerges as the right choice. Recall that the inertial effects are responsible for the destabilizing action in the present problem while the capillary force opposes this destabilizing effect. At the typical liquid saturations encountered near the trickling-to-pulsing transitions in trickle beds, the magnitude of $J'$ corresponding to the drainage curve is smaller than that corresponding to the imbibition curve or any other curve lying between the drainage and the imbibition curves. Therefore, the drainage curve predicts a lower stabilizing capillary force than any other curve. Consequently, it is hardly surprising that $J$-function corresponding to the drainage curve predicts loss of stability before any other curve for the $J$-function.

## Loss of Existence of Steady-State Solution

A major assumption embodied in the model for trickling-to-pulsing transition described earlier is that the gas phase may be treated as incompressible. At low pressure drops the gas phase density may be treated as constant and there will be little dependence of the fluid velocities or liquid holdup on axial position. This is likely to be the case for a wide range of operating conditions in the trickling flow regime, and in fact, this type of analysis was used by Saez and Carbonell (1985) to correlate pressure drop and liquid holdup data in trickle bed reactors. At high gas flow rates the pressure in the gas phase will be a strong function of axial position, resulting in corresponding changes in liquid holdup, and velocities of gas and liquid. As the gas and liquid flow rates are raised from low values, to values close to the limit of the pulsing flow regime, the formation of pulses in laboratory scale columns can first be observed at the bottom of the packed bed. The top portion of the packed column still exhibits trickle flow behavior, but an obvious change occurs near the column exit as the pulses develop. When the liquid and gas flow rates are raised further in the pulsing flow regime, the point of incipient pulsing moves up the packed bed. This evidence seems to point to the formation of large axial liquid holdup gradients as the pulsing flow regime is approached. In this section we shall describe an analysis of the steady-state volume averaged equations of motion for the two-phase flow in trickle beds, in which the gas phase will be treated as compressible. Axial variations in velocities and liquid holdup under trickling flow conditions will emerge naturally in such an analysis. It will become apparent that steady-state solutions may not exist for certain operating conditions. [It is interesting to note that a similar situation arises in the context of one-dimensional flow of gas and solid particles in a vertical standpipe (Ginestra et al., 1980; Rangachari and Jackson, 1982).] In the context of trickle beds, the absence of a steady-state solution may imply the onset of a time-dependent solution, i.e., trickling-to-pulsing transition. Such a physical model for the transition mechanism is very different from the one described earlier. We emphasize that in a complex problem such as trickle bed hydrodynamics the transition from trickling to pulsing may arise as a result of more than one transition mechanism. Hence, it is important to investigate the various possible transition mechanisms and identify that transition mechanism yielding the onset of a time-dependent solution soonest as one increases the gas and liquid flow rates.

For the case of steady, one-dimensional downward flow of the gas and the liquid, Eqs. 9, 11, 12, 13 and 15 describe continuity, momentum balance and the (approximate) stress balance at the gas-liquid interface. As in the previous section, we shall neglect the viscous and pseudoturbulence terms in Eq. 12. It can be shown after some algebraic manipulations that

$$W_4 \frac{d\epsilon_l}{dz} - \left(\frac{G^2\gamma_g}{\rho_g \epsilon_g^2}\right)\frac{dp_g}{dz} = \frac{F_{lz}}{\epsilon_l} - \frac{F_{gz}}{\epsilon_g} + (\rho_g - \rho_l)g \qquad (39)$$

$$\left[1 - \frac{G^2\gamma_g}{\rho_g \epsilon_g^2}\right]\frac{dp_g}{dz} + \frac{G^2}{\rho_g \epsilon_g^3}\frac{d\epsilon_l}{dz} = \frac{F_{gz}}{\epsilon_g} + \rho_g g \qquad (40)$$

where we have allowed for the compressibility of the gas phase and assumed isothermal conditions. $W_4$ in Eq. 39 has been defined earlier in Eq. 32. The isothermal compressibility of the gas phase, $\gamma_g$, is defined as

$$\gamma_g = -\rho_g [d(1/\rho_g)/dp_g]_T.$$

For an ideal gas phase,

$$\rho_g = M_g p_g / RT$$

where $M_g$ is the molecular weight of the gas, $R$ is the gas constant, and $T$ is the temperature of the gas. Eqs. 39 and 40 will have to be integrated to compute the steady-state liquid holdup and gas phase pressure as a function of position in the column, once suitable boundary conditions have been specified. For boundary conditions, we shall assume the gas phase pressure to be known (say, atmospheric) at the bottom of the column, while the liquid holdup at this location will be evaluated by solving Eq. 17 (the gas phase density required for solving this equation being estimated at the exit pressure).

When numerical integration of Eqs. 39 and 40 with the above

boundary conditions was attempted, it was found that solutions could not be obtained under certain operating conditions. Inspection of the numerical results for a variety of cases revealed that the key quantity which determined whether a steady-state solution existed or not is $W_4$, which appears in Eq. 39. The numerical integration of Eqs. 39 and 40 yielded meaningful solution only if $W_4$ was less than zero everywhere in the column. [A more rigorous criterion would be that the determinant of the coefficients in the LHS of Eqs. 39 and 40 must be negative. But, for practical purposes, this rigorous criterion is almost indistinguishable from the simpler result that $W_4$ be less than zero.] Under conditions of low gas and liquid flow rates, the capillary term in $W_4$ was larger than the sum of the inertial terms and $W_4$ was less than zero at all axial positions. This gave stable numerical solutions. Under such cases, the liquid holdup increases slightly as one moves up the column. Figure 3 illustrates the axial variation of liquid holdup in a 10 m long bed. The sum of the inertial terms in $W_4$ was largest at the bottom of the bed. This was due to the expansion of the gas phase in going from a higher pressure at the top of the column, to atmospheric pressure at the bottom of the column. The capillary term in $W_4$ was also larger at the bottom of the column than anywhere else in the column. This was due to the fact that the liquid holdup decreased from the top to the bottom of the packed bed, Figure 1. Note in Figure 3 that the liquid holdup gradients are very small even under high gas and liquid flow rate conditions. Changes in the liquid holdup of this order of magnitude would be difficult (if at all possible currently) to measure experimentally.

It is important to note that these gradients in liquid holdup and gas-phase pressure are driven by the compressibility of the gas phase. When the gas and liquid flow rates exceeded some critical values, no stable numerical solution could be obtained. This could happen in one of two ways. First, it could turn out that $W_4$ is greater than or equal to zero at the bottom of the column. Second, it could be possible that $W_4$ is negative at the bottom of the column, but vanished somewhere in the column. At a constant gas flow rate as one increases the liquid flow rate (or vice versa), the second possibility stated above was observed to occur first in simulations performed with a column length of 10 m (Grosser, 1988), and thus the length of the packed column can become a consideration in locating the gas and liquid flow rate combinations beyond which no stable numerical solutions could be obtained for the steady-state equations. However, simulations performed with a column length of 1 m (which is typical of a laboratory scale unit) revealed that the critical $L$ and $G$ combinations beyond which no stable numerical solution could be found for Eqs. 39 and 40 are essentially indistinguishable from those for which $W_4$ was equal to zero at the bottom of the column. Thus, one may state with reasonable accuracy that the conditions of trickling-to-pulsing transition in laboratory scale units according to this model, are given by

$$W_4 = 0 \tag{41}$$

at the column exit.

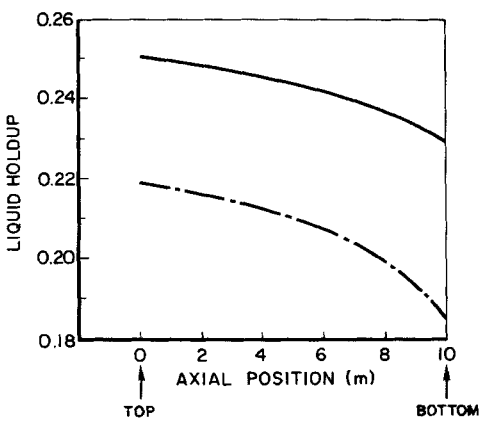


**Figure 3. Dependence of the liquid holdup on the axial position in 10-m-long packed bed for two different sets of flow rates.**

$L = 25$ kg/m$^2$ · s; —, $G = 0.17$ kg/m$^2$ · s; – – –, $G = 0.69$ kg/m$^2$ · s.

## Model Comparisons

It is instructive to compare the criteria for trickling-to-pulsing transition as deduced from the two models discussed thus far. According to the linear stability analysis described previously (henceforth Model I), the onset of pulsing is described by Eq. 37, while the analysis based on the compressibility of the gas phase described earlier (henceforth Model II) leads to Eq. 41 as the criterion for trickling-to-pulsing transition. It is not difficult to see that $W_1 > 0$; for cocurrent downflow $W_3 > 0$; and for the constitutive models described by Eqs. 5 and 6, $W_2 > 0$, and $W_5 < 0$. It follows immediately that Model I will predict the transition from trickling to pulsing at lower $L$ and $G$ values than Model II, for a given set of values for the physical properties. In other words, *the loss of stability of a steady state* in trickling flow regime is predicted to *occur before the loss of existence of a steady-state solution.* Of course, one should *not* interpret from the above argument that the compressibility of the gas phase is *not* a significant consideration in the trickling-to-pulsing transition. The linear stability analysis described earlier could, for example, be extended by allowing for the compressibility of the gas phase. Such an extension renders the analysis extremely tedious and will not be examined in this paper.

The effect of interfacial tension on the trickling-to-pulsing transition is illustrated in Figure 4. Shown in this figure are the predictions of the two models described in this paper and the microscopic model of Ng (1986), along with the experimental data of Chou et al. (1977) for two different values of interfacial tension. [In order to compute the trickling-to-pulsing transition according to the microscopic model of Ng (1986), one must first estimate the value of steady-state liquid holdup for the specified L and G values. To be consistent with the models presented in this paper, we have used the value of liquid holdup obtained by solving Eq. 17 as an input for the microscopic model.] All three models predict that the transition to pulsing will occur at lower flow rates when the interfacial tension is decreased, in qualitative agreement with the experimental trends. However, none of the models is in quantitative agreement with the experimental data. The predictions of Model I are much closer to the experimental data than those of the other two models.

The effect of bed porosity on the tricking-to-pulsing transition is presented in Figure 5. All the three models predict that an increase in bed porosity from 0.36 to 0.40 will result in a shift of the transition locus to higher flow rates, in qualitative agree-

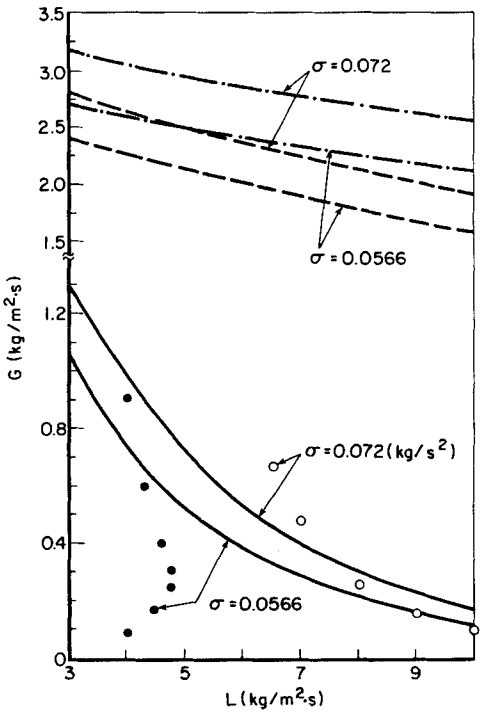


**Figure 4. Effect of interfacial tension on the trickling-to-pulsing transition locus.**

Bed porosity, $\epsilon = 0.40$; particle diameter, $d_e = 3$ mm. The values of other parameters are given in Table 1. —, Model I; – – –, Model II; – · –, Ng (1986); ●, O, Chou et al. (1977).

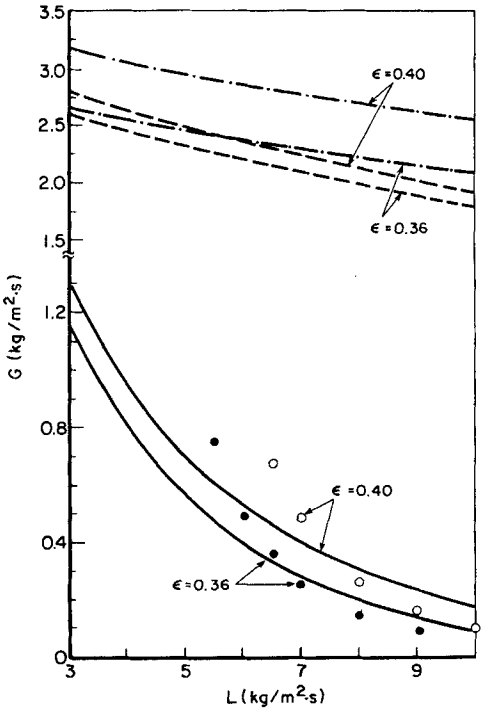


**Figure 5. Effect of bed porosity on the trickling-to-pulsing transition locus.**

$d_e = 3$ mm; $\sigma = 0.0715$ kg/s². The values of other parameters are in Table 1. —, Model I; – – –, Model II; – · –, Ng (1986); ●, O, Chou et al. (1977).

ment with the experimental trends. As in Figure 4, the predictions of Model I are much closer to the experimental data than those of the other two models.

Figure 6 shows the effect of the size of the packing particles on the transition locus, as predicted by the three models. Chou et al. (1977) found that at low liquid flow rates, the critical gas flow rate at which the transition occurred decreased with increasing particle size. However, at high liquid flow rates no discernible trend could be observed in the manner in which the particle size affected the transition locus. Model II and the microscopic model of Ng (1986) predict a very sharp decrease in the flow rates at which the onset of pulsing will occur, as the particle size is decreased. For $d_e = 8$ mm, the microscopic model predicts that the two-phase cocurrent downflow is unstable everywhere. The predictions of Model I appear to reflect the experimental trends reasonably well.

As mentioned in the Introduction, the transition from trickling to pulsing has been studied experimentally by a number of researchers. It has become a practice to present the experimental data in the form of a plot (or correlation) of $[L\lambda\psi/G]$ as a function of $[G/\epsilon\lambda]$ where

$$\lambda = [\rho_g \rho_\ell / \rho_{\text{water}} \rho_{\text{air}}]^{1/2}$$

$$\psi = \left[\frac{\sigma_{\text{water}}}{\sigma_\ell}\right]\left[\left(\frac{\mu_\ell}{\mu_{\text{water}}}\right)\left(\frac{\rho_{\text{water}}}{\rho_\ell}\right)^2\right]^{1/2}$$

Such correlations do not account for all the parameters (for example, particle size), and even those parameters which are included through the groups $\psi$ and $\lambda$ are not taken into account in an entirely satisfactory manner. As a result there is a substan-

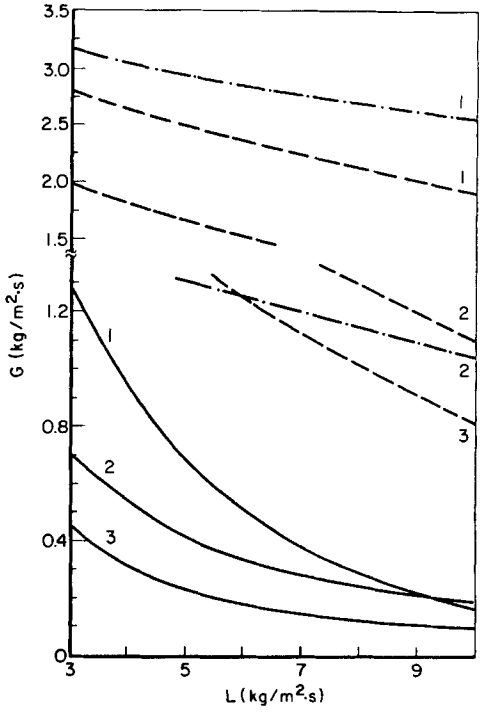


**Figure 6. Effect of particle size on the trickling-to-pulsing transition.**

$\epsilon = 0.40$; $\sigma = 0.0715$ kg/s². 1) $d_e = 3$ mm; 2) $d = 6$ mm; 3) $d_e = 8.0$ mm. The values of other parameters are shown in Figure 1.

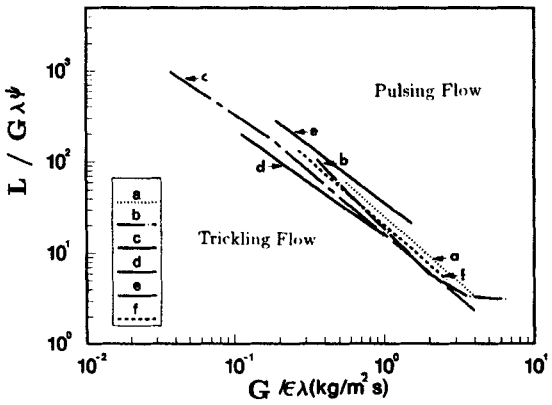


**Figure 7. Flow regime transition.**
Experimental data (Gianetto et al., 1978). See Table 2 for legends.

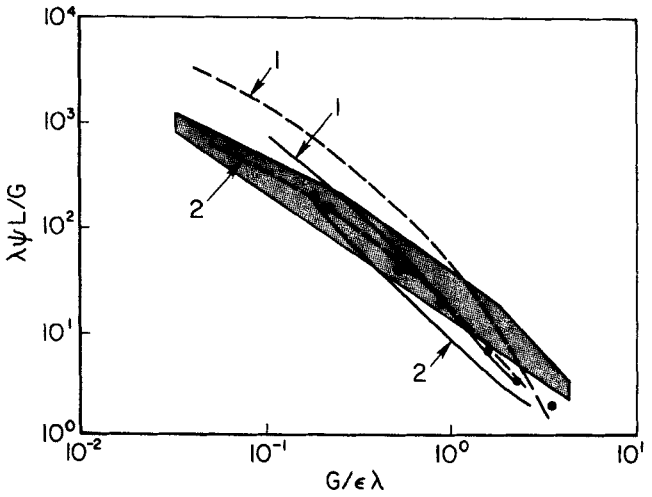


**Figure 8. Trickling-to-pulsing transition.**
The shaded region represents the experimental data of various researchers. Also shown are the predictions of Models I and II for the air-water system. — 1), Model I for $d_e$ = 6 mm, $\epsilon$ = 0.4; — 2), Model I for $d_e$ = 8 mm, $\epsilon$ = 0.4; – – – 1), Model II for $d_e$ = 6 mm, $\epsilon$ = 0.4; – – – 2), Model II for $d_e$ = 8 mm, $\epsilon$ = 0.4; ● are obtained from Model I for $d_e$ = 3 mm and $\epsilon$ = 0.37.

tial scatter in the data presented in this form. This is illustrated in Figure 7. The liquids, gases and packings corresponding to the experimental lines shown in this flow map are presented in Table 2. Note that a wide range of liquids, gases and packings were used by the different investigators, yielding a wide range of transition lines. No real trends emerge with respect to particle diameter or shape. The transition lines shown in Figure 7 are those summarized by Gianetto et al. (1978).

The shaded region in Figure 8 is where most of the experimental data of various researchers (Figure 7) lie. The experimental data are shown in Figure 8 as a shaded region for reasons of clarity of presentation. Also shown in Figure 8 are the predictions of Models I and II described in the present study for different particle diameters and bed porosities. The gross trends predicted by both models are in qualitative agreement with the bulk of the experimental data.

The models described in this paper are certainly not based completely on first principles. Empiricism enters the analysis through constitutive models for the capillary pressure and the drag force terms (Eqs. 5, 6 and 38). It is important to consider the sensitivity of the model predictions with respect to the numerical values of the constants and exponents appearing in these constitutive models. The location of the trickling-to-pulsing transition predicted by the models were found to be only a weak function of the constants and exponents in the constitutive models for the drag forces. On the other hand, it is very sensitive function of the coefficient in front of the logarithmic function in Eq. 38 which was used as the constitutive model for the capillary pressure. Had this coefficient been about a factor of ten lower, then the predictions of Model II described previously would have been very close to most of the experimental data discussed in Figures 4 to 6, and Model I would have predicted transition to occur at $G$ and $L$ combinations much lower than the experimentally observed values. This point serves to emphasize the need for more (experimental) work to characterize capillary forces

**Table 2. Legends for Figure 7**

| Curve | Reference | Size (mm) | Packing Type | $\epsilon$ | Gas | Liquid |
|---|---|---|---|---|---|---|
| a | Gianetto et al. (1970) | 6 | Glass Spheres | 0.41 | Air-NaOH | Water |
| | | 6 | Glass Rings | 0.71 | Air-NaOH | Water |
| | | 6 | Ceramic Rings | 0.50 | Air-NaOH | Water |
| | | 6 | Berl Saddles | 0.59 | Air-NaOH | Water |
| b | Sato et al. (1973) | 8 | Glass Spheres | 0.39 | Air | Water |
| c | Charpentier et al. (1975) | 3 | Catalyst Spheres | 0.39 | Air | Water |
| | | 1.8 × 6 | Catalyst Cylinders | 0.39 | Air | Water |
| | | 1.4 × 5 | Catalyst Cylinders | 0.37 | $N_2$ | $C_6H_{12}$ |
| | | 1.4 × 5 | Catalyst Cylinders | 0.37 | $CO_2$ | Gasoline |
| | | 1.4 × 5 | Catalyst Cylinders | 0.37 | *He* | Gasoline |
| d,e | Chou et al. (1976) | 2.9 | Glass Beads | 0.39 | Air | EtOH-$H_2O$ |
| | | 2.9 | Glass Beads | 0.39 | Air | MeOH-$H_2O$ |
| | | 2.9 | Glass Beads | 0.39 | Air | Aq. Surfactants |
| f | Specchia et al. (1977) | 6 | Glass Beads | 0.40 | Air | Water |
| | | 5.4 × 5.4 | Glass Cylinders | 0.37 | Air | Water |
| | | 5.4 × 5.4 | Glass Cylinders | 0.37 | Air | Glycerol Aq. |
| | | 2.7 × 2.7 | Glass Cylinders | 0.38 | Air | $H_2O$ |

under flow conditions in trickle beds, before definitive statements can be made about the mechanism of transition from trickling to pulsing.

At the present time, if we assume that Leverett's data on capillary pressures in porous media can be employed in the context of two-phase flow through trickle beds, Model I which is based on the loss of stability of a state of uniform trickling appears to describe the transition from trickling to pulsing more satisfactorily than any other model.

## Summary

During cocurrent downflow of a gas and a liquid through a packed column, a state referred to as trickling flow is obtained at low gas and liquid flow rates. Quantities such as the liquid holdup, pressure gradient, etc. are essentially independent of time in this state of trickle flow. As one increases the flow rates of the gas and/or the liquid, a transition from this steady trickling flow to a time-dependent flow behavior known as pulsing is obtained. The conditions at which this instability sets in is analyzed by using a simple macroscopic model for the two-phase flow.

If we treat the gas phase as incompressible, the hydrodynamic model admits a uniform solution for given gas and liquid flow rates. A criterion for the onset of pulsing is derived by examining the linear stability of this uniform state. Physically, the inertial effects tend to destabilize the uniform state while the capillary action counteracts the inertial effects. At sufficiently high flow rates, the inertial effects become dominant and the pulsing flow is obtained.

In reality, the gas expands as it flows through the column. This results in a small axial variation of the liquid holdup. Under certain operating conditions, one encounters a scenario where no solutions exist for the steady-state, macroscopic model for the two-phase flow. A simple criterion for this situation is presented.

The conditions at which loss of stability of the uniform state (treating the gas phase as incompressible) occur are the conditions at which the loss of existence of steady solutions occur are compared with experimental data on trickling-to-pulsing transition. The former appears to be a more reasonable explanation.

## Notation

$A, B$ = Ergun constants
$d_e$ = particle diameter
$E\ddot{o}$ = Eotvos number (see Eq. 7)
$\underline{F}_i$, $i = \ell, g$ = total drag force per unit bed volume experienced by phase $i$
$F_{iz}$, $i = \ell, g$ = drag force per unit bed volume experienced by phase $i$ in the axial direction.
$g$ = acceleration due to gravity
$G$ = gas-phase mass flux
$J(\epsilon_\ell)$ = Leverett $J$ function
$J'(\epsilon_\ell) = dJ/d\epsilon_\ell$
$k$ = permeability of the packed column
$L$ = liquid-phase mass flux
$M_g$ = molecular weight of the gas
$p_i$, $i = \ell, g$ = pressure in phase $i$
$p_{i1}, \hat{p}_{i1}$, $i = \ell, g$ = see Eqs. 20 and 27
$p_c$ = capillary pressure
$\underline{\underline{R}}_i$, $i = \ell, g$ = pseudoturbulence stress tensor for phase $i$
$R$ = gas constant
$s_\ell = \epsilon_\ell/\epsilon$
$s'_\ell = \epsilon'_\ell/\epsilon$
$t$ = time
$T$ = temperature
$u_i$, $i = \ell, g$ = velocity of phase $i$
$u_{i1}, \hat{u}_{i1}$, $i = \ell, g$ = see Eqs. 20 and 27
$W_1$-$W_5$ = see Eqs. 28–33

### Greek letters

$\alpha_i, \beta_i$, $i = \ell, g$ = see Eq. 26
$\gamma_g$ = isothermal compressibility of the gas
$\epsilon$ = porosity of the bed
$\epsilon_i$, $i = \ell, g$ = volume fraction of phase $i$ in the bed
$\epsilon'_\ell$ = residual liquid holdup
$\epsilon_{i1}, \hat{\epsilon}_{i1}$, $i = \ell, g$ = see Eqs. 20 and 27
$\rho_i$, $i = \ell, g$ = density of phase $i$
$\mu_i$, $i = \ell, g$ = viscosity of phase $i$
$\sigma$ = interfacial tension
$\underline{\underline{\tau}}_i$, $i = \ell, g$ = viscous stress tensor for phase $i$
$\omega$ = wavenumber

### Superscript

0 = uniform steady state

## Literature Cited

Beimesch, W. E., and D. P. Kessler, "Liquid-Gas Distribution Measurements in the Pulsing Regime of Two-Phase Concurrent Flow in Packed Beds," *AIChE J.*, **17**, 1160 (1971).

Baker, O., "Simultaneous Flow of Oil and Gas," *Oil Gas J.*, **53**(12), 185 (1954).

Blok, J. R., and A. A. H. Drinkenburg, "Hydrodynamic Properties of Pulses in Two-Phase Downflow operated Packed Columns," *Chem. Eng. J.*, **25**, 89 (1982a).

Blok, J. R., and A. A. H. Drinkenburg, "Hydrodynamics and Mass Transfer in Pulsing Trickle Bed Columns," *Chem. Rxn. Eng., A.C.S. Symp. Ser.*, No. 190, 393 (1982b).

Blok, J. R., J. Varkevisser, and A. A. M. Drinkenburg, "Transition to Pulsing Flow, Holdup and Pressure Drop in Packed Columns with Cocurrent Gas-Liquid Downflow," *Chem. Eng. Sci.*, **38**, 687 (1983).

Charpentier, J. C., "Recent Progress in Two-Phase Gas-Liquid Mass Transfer in Packed Beds," *Chem. Eng. J.*, **11**, 161 (1976).

Charpentier, J. C., M. Bakos, and P. LeGoff, *Proc. Int. Cong.*, Vesprem, Hungary (Aug. 2–5, 1971).

Charpentier, J. C., and M. Favier, "Some Liquid Holdup Experimental Data in Tricke-Bed Reactors for Foaming and Nonfoaming Hydrocarbons," *AIChE J.*, **21**, 1213 (1975).

Christensen, G., S. J. McGovern, and S. Sundaresan, "Concurrent Downflow of Air and Water on a Two-Dimensional Packed Column," *AIChE J.*, **32**, 1677 (1986).

Chou, T. S., F. L. Worley, and D. Luss, "Transition to Pulsing Flow in Mixed-Phase Cocurrent Downflow through a Fixed Bed," *Ind. Eng. Chem. Process Des. Dev.*, **16**, 424 (1977).

Dullien, F. A. L., *Porous Media: Fluid Transport and Pore Structure*, Academic Press (1979).

Fukushima, S., and K. J. Kusaka, "Interfacial Area and Boundary of Hydrodynamic Flow Regions in Packed Column with Cocurrent Downward Flow," *J. Chem. Eng. Japan*, **10**, 461 (1977).

Gianetto, A., G. Baldi, V. Specchia, and S. Sicardi, "Hydrodynamics and Solid-Liquid Contacting Effectiveness in Trickle-Bed Reactors," *AIChE J.*, **24**, 1087 (1978).

Gianetto, A., V. Specchia, and G. Baldi, "Absorption in Packed Towers with Concurrent Downward High-Velocity Flows II: Mass Transfer," *AIChE J.*, **19**, 916 (1973).

Ginestra, J. C., S. Rangachari, and R. Jackson, "A One-Dimensional Theory of Flow in a Vertical Standpipe," *Powder Tech.*, **27**, 69 (1980).

Grosser, K. A., Ph.D. Dissertation, Chemical Engineering Dept., North Carolina State Univ., Raleigh, NC (1988).

Herskowitz, M., and J. M. Smith, "Trickle-Bed Reactors: A Review," *AIChE J.*, **29**, 1 (1983).

Kan, K. M., and P. F. Greenfield, "Pressure Drop and Holdup in Two-Phase Cocurrent Trickle Flows through Beds of Small Particles," *Ind. Eng. Chem. Process Des. Dev.*, **18**, 760 (1979).

Kan, K. M., and P. F. Greenfield, "Multiple Hydrodynamic States in Cocurrent Two-Phase Downflow through Packed Beds," *Ind. Eng. Chem. Process Des. Dev.*, **17**, 482 (1978).

Kobayashi, S., S. Kushiyama, Y. Ida, and N. Wakao, "Flow Characteristics in Axial Dispersion in Two-Phase Downflow in Packed Columns," *Kagaku Kogaku Ronbunshu,* **5,** 256 (1979).
Larkins, R. P., R. R. White, and D. W. Jeffrey, "Two-Phase Concurrent Flow in Packed Beds," *AIChE J.,* **7,** 231 (1961).
Lerou, J. J., D. Glasser, and D. Luss, "Packed bed Liquid Phase Dispersion in Pulsed Gas-Liquid Downflow," *Ind. Eng. Chem. Fund.,* **19,** 66 (1980).
Levec, J., K. Grosser, and R. G. Carbonell, "Experimental Observations on the Hysteretic Behavior of the Liquid Holdup and Pressure Drop in Trickle Beds," *AIChE J.,* **34,** 6 (June, 1988).
Levec, J., A. E. Saez, and R. G. Carbonell, "Holdup and Pressure Drop in Trickle-Bed Reactors," *Int. Symp. Chem. React. Eng.,* Edinburgh (1984).
Levec, J., A. E. Saez, and R. G. Carbonell, "The Hydrodynamics of Trickling Flow in Packed Beds: II. Experimental Observations," *AIChE J.,* **32,** 369 (1986).
Leverett, M. C., "Capillary Behavior in Porous Solids," *Trans. AIME,* **142,** 159 (1941).
Midoux, N., M. Favier, and J. C. Charpentier, "Flow Pattern, Pressure Loss, and Liquid Holdup Data in Gas-Liquid Downflow Packed Beds with Foaming and Nonfoaming Hydrocarbons," *J. Chem. Eng. Japan,* **9,** 350 (1976).
Morsi, B. I., N. Midoux, and J. C. Charpentier, "Flow Pattern and Some Holdup Data in Trickle-Bed Reactors for Foaming and Nonfoaming and Viscous Organic Liquids," *AIChE J.,* **24,** 357 (1978).
Morsi, B. I., N. Midoux, A. Laurent, and J. C. Charpentier, "Hydrodynamique et Aire Interfaciale des Ecoulements Gaz-Liquide a Cocour ant ves le Bas in Lit Fixe: Influence de la Nature du Liquide," *Entropie,* **16,** 38 (1980).
Morsi, B. I., A. Laurent, N. Midoux, G. Barthole-Delauney, A. Storck, and J. C. Charpentier, "Hydrodynamics and Gas-Liquid-Solid Interfacial Parameters of Cocurrent Downward Two-Phase Flow in Trickle-Bed Reactors," *Chem. Eng. Comm.,* **25,** 267 (1984).
Ng, K. M., "A Model for Flow Regime Transitions in Cocurrent Downflow Trickle-Bed Reactor," *AIChE J.,* **32,** 115 (1986).
Rangachari, S., and R. Jackson, "The Stability of Steady States in a One-Dimensional Model of a Standpipe Flow," *Powder Tech.,* **31,** 185 (1982).
Saez, A. E. and R. G. Carbonell, "Hydrodynamic Parameters for Gas-Liquid Cocurrent Flow in Packed Beds," *AIChE J.,* **31,** 52 (1985).
Sato, Y., T. Hirosa, F. Takahashi, M. Toda, and Y. Hashiguchi, "Flow Pattern and Pulsation Properties of Cocurrent Gas-Liquid Downflow in Packed Beds," *J. Chem. Eng. Japan,* **6,** 315 (1973).
Satterfield, C. N., "Trickle-Bed Reactors," *AIChE J.,* **21,** 209 (1975).
Scheidegger, A. E., *The Physics of Flow Through Porous Media,* 3rd ed., Univ. of Toronto Press (1974).
Schmidt, P. C., and L. D. Clements, "Two-Phase Downflow through Catalysts Beds: Part II:—Pulsing Regime Pressure Drop," *AIChE J.,* **23**(6), 874 (1977).
Sicardi, S., M. Gerhard, and M. Hoffmann, "Flow Regime Transition in Trickle-Bed Reactors," *Chem. Eng. J.,* **18,** 173 (1979).
Sicardi, S., and H. Hoffmann, "Influence of Gas Velocity and Packing Geometry on Pulsing Inception in Trickle-Bed Reactors," *Chem. Eng. J.,* **20,** 251 (1980).
Specchia, V., S. Sicardi, and A. Gianetto, "Absorption in Packed Towers with Concurrent Upward Flow," *AIChE J.,* **20,** 646 (1974).
Specchia, V., and G. Baldi, "Pressure Drop and Liquid Holdup for Two-Phase Concurrent Flow in Packed Beds," *Chem. Eng. Sci.,* **32,** 515 (1977).
Talmor, E., "Two-Phase Downflow through Catalyst Beds: I. Flow Maps," *AIChE J.,* **23,** 868 (1977).
Tosun, G., "A Study of Cocurrent Downflow of Nonfoaming Gas-Liquid Systems in a Packed Bed: 1. Flow Regimes: Search for a Generalized Flow Map," *Ind. Eng. Chem. Process Des. Dev.,* **23,** 29 (1984).
Turpin, J. L., and R. L. Huntington, "Prediction of Pressure Drop for Two-Phase, Two-Component Concurrent Flow in Packed Beds," *AIChE J.,* **13,** 1196 (1967).
Weekman, Jr., V. W., and J. E. Myers, "Fluid Flow Characteristics of Cocurrent Gas-Liquid Flow in Packed Beds," *AIChE J.,* **10,** 951 (1964).

*Manuscript received Feb. 5, 1988, and revision received June 2, 1988.*